An ^{1}H NMR Microimaging Visualization of Hexachloroplatinate Dianion Redistribution within a Porous γ-Al_2O_3 Pellet in the Course of Supported Catalyst Preparation

L. Yu. Khitrina,[†] I. V. Koptyug,*[,‡] N. A. Pakhomov,[†] R. Z. Sagdeev,[‡] and V. N. Parmon[†]

Boreskov Institute of Catalysis, Acad. Lavrentiev pr. 5, Novosibirsk 630090, Russia, and International Tomography Center, Institutskaya str. 3A, Novosibirsk 630090, Russia

Received: December 15, 1999

The application of the ^{1}H NMR microimaging technique to the indirect mapping of the spatial distribution of hexachloroplatinate dianion within porous alumina pellets is reported. It is demonstrated that the nuclear spin−lattice relaxation times of liquids filling the pores of the pellet increase in the presence of the adsorbed hexachloroplatinate dianion. The microimaging results for the supported catalysts with two types of platinum distribution (egg-shell and egg-white) are shown to be consistent with the results obtained by the staining method and electron probe microanalysis. Finally, the microimaging technique is employed for a nondestructive visualization of the dynamics of the active component redistribution in the course of the supported catalyst preparation by competitive adsorption.

Introduction

One of the most important characteristics of supported catalysts is the type of the macroscopic distribution of an active component within the support. Four ultimate distribution types are commonly distinguished: uniform, egg-shell, egg-white, and egg-yolk.[1−3] For each particular catalyst the preferable distribution type is determined by a number of practical aspects of its use in a catalytic process, such as the location of the reaction zone within the pellet, the possibility of catalyst wear, the activity of catalyst poisons, etc. Therefore, the information about the distribution type, its dependence on the properties of the support and the impregnated substance, and the ability to control the distribution type are essential for supported catalyst preparation.

A variety of conventional techniques is available for the visualization of the active component distributions; these include electron probe microanalysis,[4,5] scanning microscopy,[6] autoradiographic[7] and light transmission[5] techniques, and staining methods.[8] Since all these techniques are destructive, the studies of the dynamics of the active component redistribution upon preparation of supported catalysts are performed by interrupting the impregnation process at different stages and require a large number of pellets. This is obviously a laborious and time-consuming task, which is not absolutely reliable due to the variation of the porous structure even within one batch of the support pellets.

The ability of ^{1}H NMR microscopy to indirectly map the distribution of adsorbates within porous supports is based on the sensitivity of the relaxation times of liquids filling the pores to the presence of adsorbed substances. The relaxation times can change by several orders of magnitude when paramagnetic adsorbates are used,[9] but even for the nonparamagnetic substances the change can be observable. The relaxation times of water within an alumina pellet were used to map the distribution of coke formed in the ethanol dehydration reaction.[10]

The results of the present study demonstrate the ability of the ^{1}H NMR microscopy to reveal nondestructively the spatial distribution of the adsorbed hexachloroplatinate dianion ($PtCl_6^{2-}$) within the catalyst pellets, and to map its redistribution in a single support pellet in real time without the need to interrupt the impregnation process. The choice of the catalyst was governed by the widespread use of this type of supported catalysts and the possibility to reliably produce the aforementioned types of distributions upon hexachloroplatinate dianion adsorption on the alumina support.

Experimental Section

Three types of cylindrical alumina (γ-Al_2O_3) pellets of different porosities were used in the experiments; their characteristics are given in Table 1. The mercury porosimetry and the low temperature (77.4 K) nitrogen adsorption measurements were performed on Micrometrics Autopore 9200 and Micrometrics ASAP 2400 instruments, respectively.

Distilled water and "purum" grade cyclohexane were used in the experiments. The active component of the catalyst (Pt) was introduced in the form of H_2PtCl_6 from a 0.02 N aqueous solution. A 0.3 N aqueous solution of oxalic acid ($H_2C_2O_4$) was used as a competitive sorbate.

For static experiments, the pellets with two types of hexachloroplatinate dianion distribution were prepared. The samples with the egg-shell distribution of hexachloroplatinate dianion (S-1, S-2, S-3) were prepared by diffusional impregnation of the pellets initially saturated with water in the absence of the competitive sorbate. The finite duration of the impregnation process (30 min in our case) is known to yield the distribution of egg-shell type.[1−3] To obtain a well-defined egg-white distribution of hexachloroplatinate dianion, the samples W-1, W-2, and W-3 were first saturated with water, then treated for 10 min with the 0.3 N oxalic acid aqueous solution, and later were placed in the 0.02 N H_2PtCl_6 + 0.3 N $H_2C_2O_4$ aqueous solution (40 min for W-1 and W-2, 1.5 h for W-3) to perform competitive adsorption. In the presence of a strongly competitive sorbate such as the oxalic acid, the hexachloroplatinate dianion is adsorbed ahead of the oxalate adsorption front and moves faster toward the pellet center. After the adsorption stage, all

* Corresponding author. E-mail: koptyug@tomo.nsc.ru. Fax: +7 3832 331399.
[†] Boreskov Institute of Catalysis.
[‡] International Tomography Center.

10.1021/jp994412+ CCC: $19.00
Published on Web 02/11/2000

TABLE 1: Specific Surface Area (A), Pore Volume (V_{pore}), and Average Pore Radius (r_{av}) of the Porous Alumina Pellets Studied in This Work

sample	nominal diameter (mm)	A^a m^2/g	V_{pore}, cm^3/g^b (∅ < 1500 Å)	V_{pore}, cm^3/g^c (∅ > 1500 Å)	r_{av}, Å^d (∅ < 1500 Å)	r_{av}, Å^c (∅ > 1500 Å)
1	5.0	236	0.63	0.21	50	9000
2	6.0	255	0.65	0.27	47	10000
3	3.6	180	0.43	0.1	40	4000

[a] BET nitrogen adsorption method. [b] Nitrogen adsorption saturation at relative nitrogen vapor pressure $P/P_s = 0.95$, where P_s is the saturated vapor pressure at ca. 77 K. [c] Mercury porosimetry. [d] Desorption branch of nitrogen adsorption isotherm.

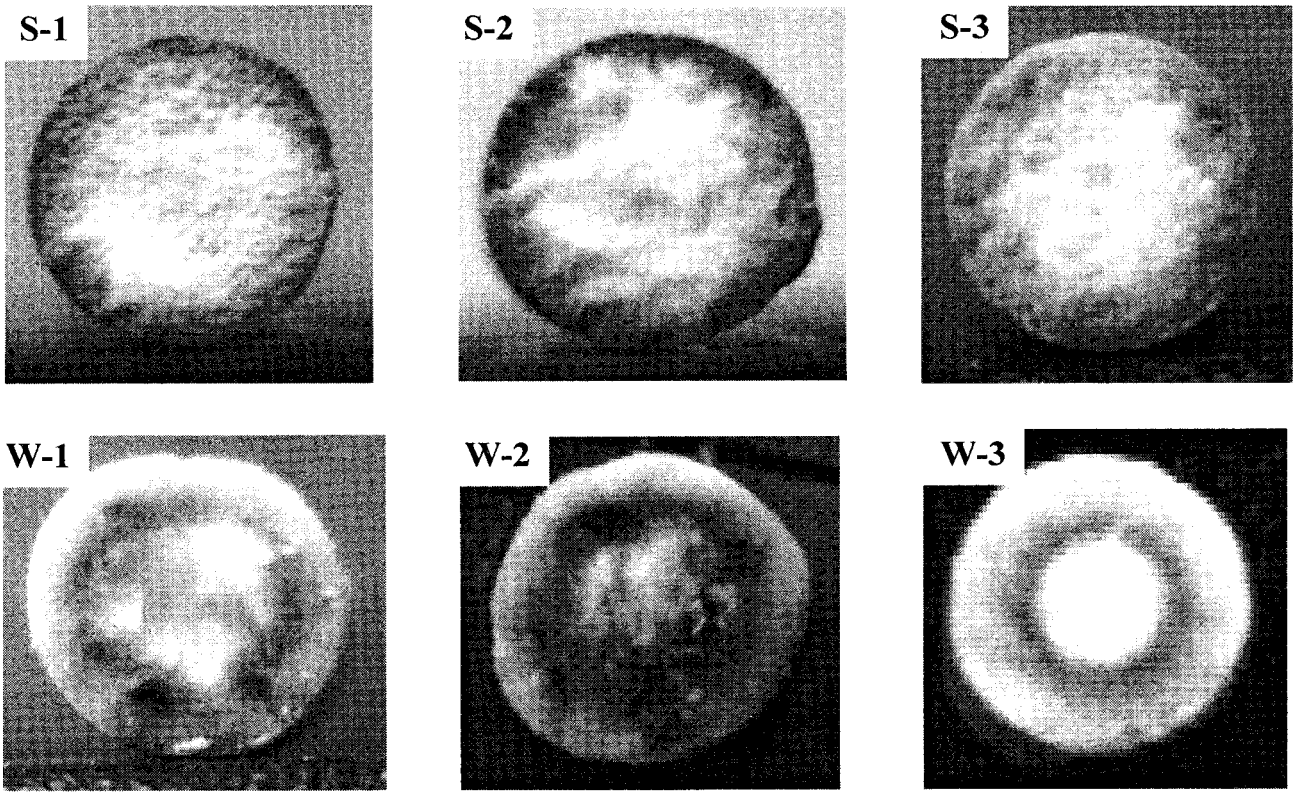

Figure 1. Digital camera photographs of the pellets' cross sections after the treatment with $SnCl_2$ for the samples with egg-shell (S-1, S-2, S-3) and egg-white (W-1, W-2, W-3) distributions of hexachloroplatinate dianion studied in this work.

samples were dried for several hours at 130 °C, and then saturated with cyclohexane. The low solubility of hexachloroplatinate in cyclohexane ensures that no redistribution of Pt occurs during the microimaging experiment. Cyclohexane exhibits a single line in the ^1H NMR spectrum, which simplifies the microimaging experiment.

For the imaging of the dynamics of hexachloroplatinate dianion redistribution in real time in the course of the impregnation process, the alumina pellet was treated with 0.3 N $H_2C_2O_4$ aqueous solution for 10 min, then it was transferred to the NMR tube containing 5 mL of 0.02 N H_2PtCl_6 + 0.3 N $H_2C_2O_4$ aqueous solution, and the imaging experiment was initiated immediately. In this case the nuclear spin relaxation times of water hydrogens are sensitive to the presence of hexachloroplatinate dianion.

All ^1H NMR microimaging experiments were performed at 300 MHz with a Bruker Avance NMR spectrometer equipped with a microimaging accessory. The cylindrical pellet was positioned inside a 10 mm NMR tube, with the axes of the sample and the tube being parallel to the main magnetic field of the superconducting magnet (z axis). In the static experiments, the pellet was wrapped around with a Teflon tape to prevent cyclohexane evaporation during image acquisition. In the dynamic imaging experiments, the cell was filled with the aqueous solution of H_2PtCl_6 + $H_2C_2O_4$.

The two-pulse spin echo sequence with inversion−recovery preconditioning and the selection of a slice ca. 3 mm thick orthogonal to the z axis in the center of the pellet was employed to detect the two-dimensional (2D) images. The delay between the pulse sequence repetitions was at least $5T_1$ to avoid any T_1-weighting other than that caused by the initial inversion pulse.

The detection of each T_1-weighted 2D image took less than 15 min of acquisition time. A set of 16 images with various degrees of T_1-weighting was obtained in about 3 h while varying the recovery delay from 2 ms to 2 s. The spatial maps of the cyclohexane spin density and the spin−lattice relaxation time were reconstructed assuming a single-exponential recovery of the signal for each individual image pixel. For many synthetic porous materials with broad distributions of pore sizes, the liquids filling the pores are characterized by a single-exponential spin−lattice relaxation as a result of fast interpore diffusion over the length scales exceeding the characteristic dimensions of the sample heterogeneity.[9] Bulk relaxation time measurements performed with the samples studied in this work are in agreement with these findings. An independent verification of the correctness of the fitting procedure employed is a high quality of the reconstructed spin density and T_1 maps obtained in this study.

For the real-time studies of the hexachloroplatinate dianion redistribution dynamics in the course of the impregnation

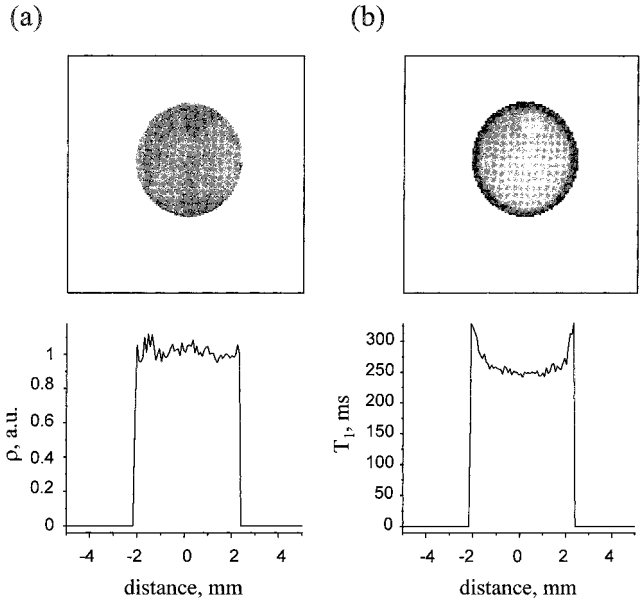

Figure 2. Proton spin density (a) and T_1 (b) maps of cyclohexane in the S-1 catalyst pellet. The size of the data matrix is 128 × 128 points, 3 mm slice thickness, pixel size = (78 μm)^2, echo time (TE) = 1.8 ms, recycle time (TR) = 2 s, number of averages (NA) = 2, field of view (FOV) = 1 cm^2.

process, a single value for the recovery delay which gave the best contrast in the T_1-weighted images (256 ms) was used. Several 2D water images were acquired sequentially after the initiation of the impregnation process; the acquisition time of each 2D image was 9 min 40 s.

Results and Discussion

Mapping the Stationary Macroscopic Distributions of Hexachloroplatinate Dianion. To verify that the preparation procedures yielded the expected Pt distributions, the cylindrical pellets of all six types prepared in this work were halved perpendicular to the cylinder axis, and their edges were treated with the hydrochloric solution of tin chloride. The latter forms colored complexes with Pt, and the color of the regions of the support containing Pt changes from light yellow to dark brown. The resulting pictures taken with a digital camera are shown in Figure 1. As can be seen in the figure, the distribution of Pt in the samples S-1, S-2, and S-3 is of egg-shell type, whereas in the samples W-1, W-2 and W-3, the active component is located in a ring-shaped area at a certain depth below the support surface, forming the egg-white type distribution. We note, however, that in the staining method the distributions can appear broader as compared to the actual ones, for the Pt−Sn complexes are weakly bound to the support and the partial redistribution of the complexes takes place after the tin chloride treatment and before the picture is taken.

Parts a and b of Figure 2 show the reconstruction results for the spatial distribution of cyclohexane spin density and its spin−lattice relaxation time for the S-1 sample. Both the two-dimensional maps (top) and their one-dimensional (1D) horizontal cross sections through the center of the pellet (bottom) are presented. Figure 2a demonstrates that the spin density distribution in the pellet is uniform, whereas the distribution of T_1 times of cyclohexane reflects the spatial distribution of hexachloroplatinate dianion within the pellet. As can be seen, the T_1 time of cyclohexane is larger in those parts of the pellet that contain adsorbed hexachloroplatinate dianion. The results of the microimaging experiments were also compared with the data obtained by the electron probe (1 μm in diameter) microanalysis for the similarly prepared samples. Figure 3 presents the two-dimensional T_1-maps, one-dimensional cross sections of these maps, and the microprobe profiles (where available) for the rest of the samples studied in this work. The microanalysis results appear to be in a reasonable agreement with the microimaging data.

The detailed mechanism which leads to the increase of the nuclear spin−lattice relaxation time of the liquid filling the pores of the alumina support impregnated with hexachloroplatinate dianion is not clear and will be studied in the future work. However, the main principles of such relaxation are well established.[11,12] The liquid-surface interactions play a predominant role in enhancing the nuclear spin relaxation of a liquid confined within the pores. The influence of the surface is twofold: it alters the mobility of the molecules in the surface layer of the liquid and also introduces additional interactions which increase the relaxation rate. Therefore, any substance adsorbed on the pore walls should in principle alter the relaxation times of the liquid by perturbing the liquid−surface interaction, the only question being whether the effect would be large enough to be observable experimentally. Another possibility is that the adsorbed substance blocks the (narrow) throats of the smaller pores, which leads to the decrease of the effective surface-to-volume ratio averaged over the sample, which seems to be in contradiction with the uniform distribution of cyclohexane in the pellets since the distribution of hexachloroplatinate dianion is nonuniform. An important observation is that the removal of chlorine atoms upon reduction of adsorbed hexachloroplatinate significantly diminishes the sensitivity of cyclohexane relaxation time to the presence of Pt.

The Dynamics of Hexachloroplatinate Dianion Redistribution. The dynamics of hexachloroplatinate dianion redistribution in the course of the competitive impregnation of the support with the aqueous solution of $H_2PtCl_6 + H_2C_2O_4$ as monitored with the NMR microimaging is presented in Figure 4. The interface between the solution and the pellet appears as a thin white ring in all images. The light ring inside the pellet corresponds to the region of adsorbed hexachloroplatinate dianion, which becomes wider and is displaced with time toward the pellet center. After ca. 5 h of impregnation, the distribution of the egg-white type transforms into the egg-yolk type distribution. At the end of the experiment, all hexachloroplatinate is adsorbed due to the limited amount of the solution used in the experiment, which is evidenced by the decoloration of the solution. There was no further redistribution of hexachloroplatinate dianion after 550 min. We stress once again that the images shown in Figure 4 were obtained without interrupting the impregnation process. The sample immersed in the solution remained inside the NMR probe during the entire experiment.

Finally, we note that no attempt was made in this work to evaluate the quantities of adsorbed Pt from the microimaging results presented above. This should await a detailed understanding of the influence of the adsorbed hexachloroplatinate dianion on the relaxation times of the liquids occupying the pores of the support. Another possibility to quantify the microimaging data is to obtain an empirical calibration of the microimaging experiment by relating the variations of the relaxation times to the local Pt quantities measured by other techniques, e.g., the electron probe microanalysis. We plan to look into these possibilities in the future studies.

Conclusions

The results of this work have demonstrated that ^{1}H NMR microimaging can be applied successfully to study the macroscopic distribution of the adsorbed hexachloroplatinate dianion

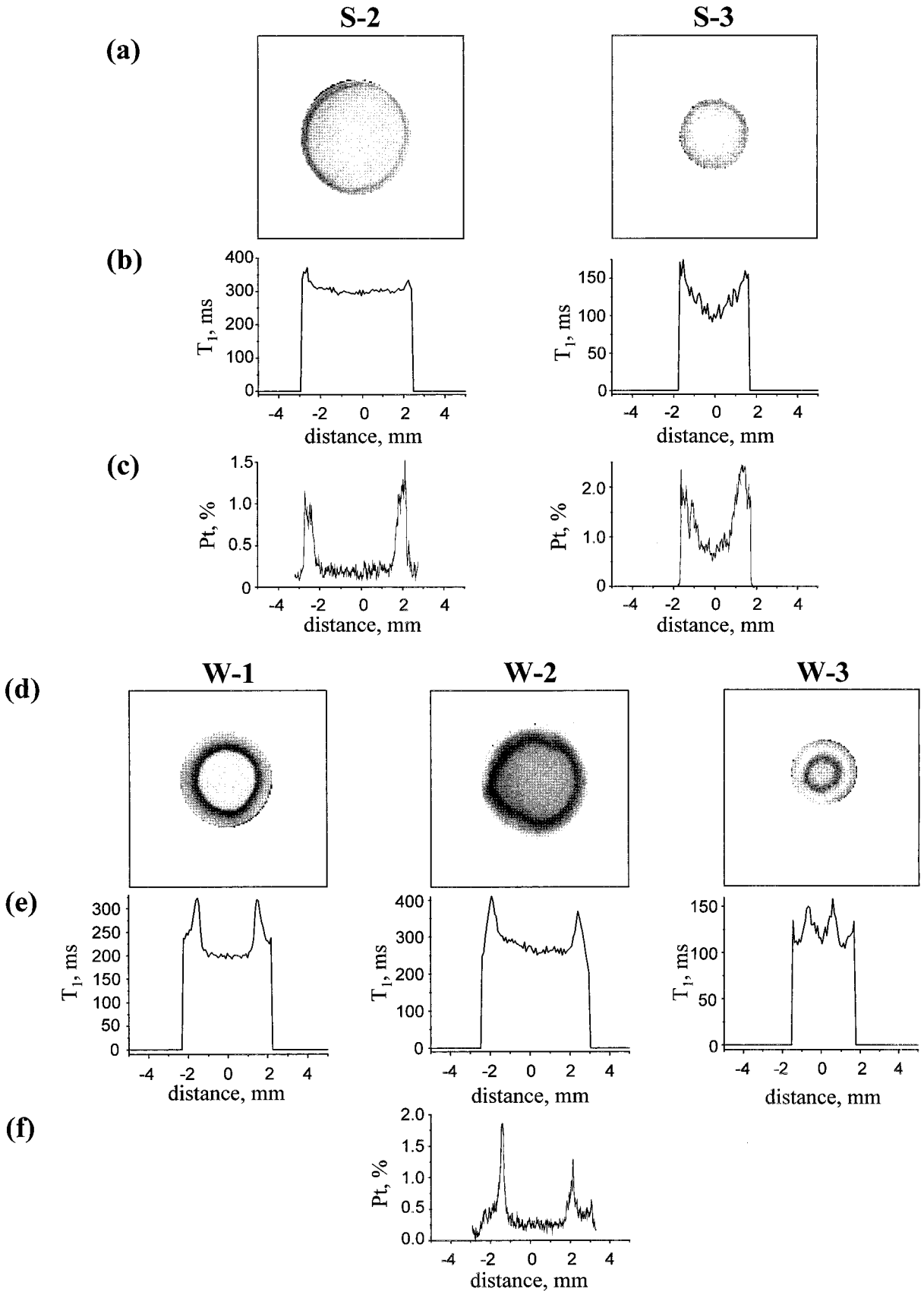

Figure 3. Two-dimensional T_1 maps (a and d), their 1D central cross sections (b and e), and the 1D profiles of hexachloroplatinate dianion distributions obtained by electron probe microanalyzer (c and f) for the samples under investigation. The parameters of the microimaging experiment are the same as in Figure 2.

within the support pellet by detecting the relaxation time weighted images of liquids filling the porous pellet. The main advantage of this technique is that, unlike with the conventional methods, the mapping is performed nondestructively. This allowed us to visualize both the stationary distributions of the active component and the real-time dynamics of its redistribution

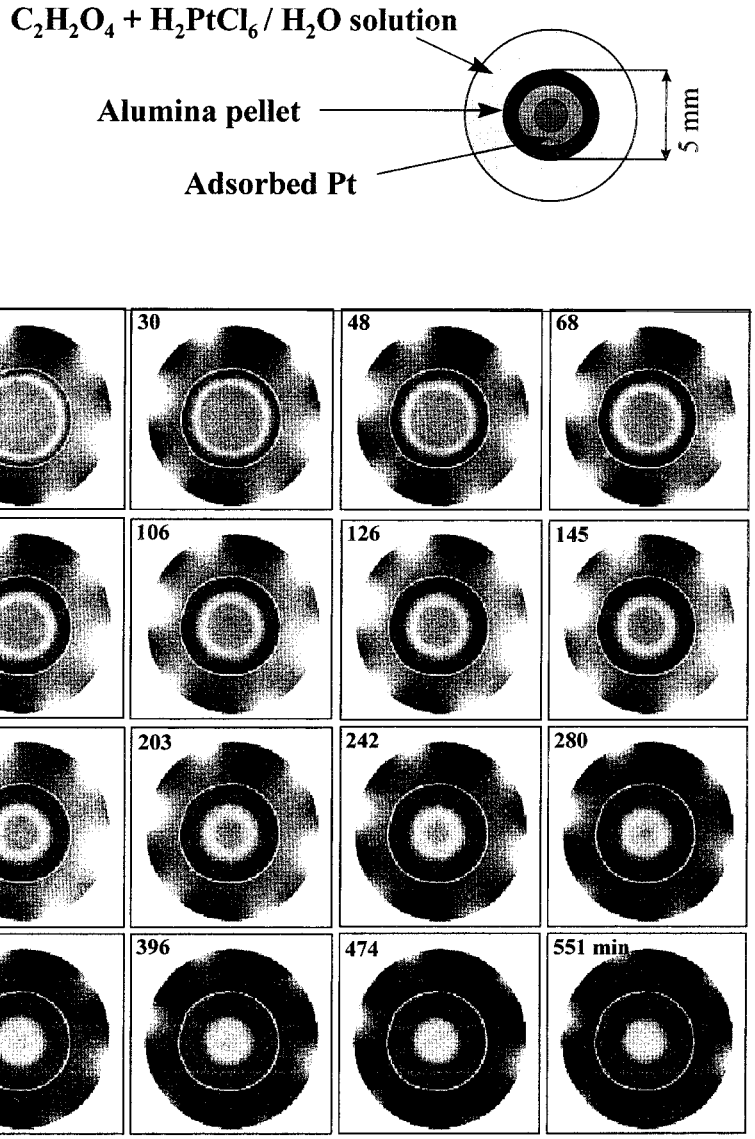

Figure 4. The dynamics of hexachloroplatinate dianion redistribution within the alumina pellet (5.0 mm nominal diameter) during the competitive impregnation with 5 mL aqueous solution of 0.02 N H_2PtCl_6 + 0.3 N $H_2C_2O_4$. The time between the start of the impregnation process and the completion of the image acquisition is given in minutes for every image. Recovery delay, 256 ms; 128 × 128 points; pixel size = (78 μm)^2; TE = 1.8 ms; TR = 2 s; NA = 2; FOV = 1 cm^2.

in the course of the supported catalyst preparation. No attempt was made in this work to evaluate the amounts of adsorbed Pt from the microimaging data; however, it can be done in principle by combining the microimaging results with the data obtained by the conventional techniques to establish the relation between the relaxation times of liquids and the amounts of adsorbed substance.

Acknowledgment. The authors thank Dr. I. A. Ovsyannikova for performing the electron probe microanalysis of Pt distribution and Prof. V. B. Fenelonov (both from the Boreskov Institute of Catalysis) for pellet texture characterization. We thank the Russian Foundation for Basic Research (Project 99-03-32314a) and the Siberian Division of the Russian Academy of Sciences for financial support of this work. L.Yu. Khitrina gratefully acknowledges a scholarship awarded by the Zamaraev International Charitable Scientific Foundation.

References and Notes

(1) Shyr, Y.-S.; Ernst, W. R. *J. Catal.* **1980**, *63*, 425.
(2) Lee, S.-Y.; Aris, R. *Catal. Rev.—Sci. Eng.* **1985**, *27*, 207.
(3) Duplyakin, V. K.; Fenelonov, V. B.; Rikhter, K.; Rodionov, A. V.; Seflut, H.; Kheifez, L. I.; Neimark, A. V.; Moskovtsev, V. V. *Fundamentals of Catalyst Technology, Proceedings of the Coordination Center*; Novosibirsk, Russia, 1981; Vol. 13, pp 137−173.
(4) Chen, H.-C.; Anderson, R. B. *J. Catal.* **1976**, *43*, 200.
(5) Komiyama, M.; Merrill, R. P.; Harnsberger, H. F. *J. Catal.* **1980**, *63*, 35.
(6) Melo, F.; Cervelló, J.; Hermana, E. *Chem. Eng. Sci.* **1980**, *35*, 2175.
(7) Harriott, P. *J. Catal.* **1969**, *14*, 43.
(8) Summers, J. C.; Hegedus, L. L. *J. Catal.* **1978**, *51*, 185.
(9) Kleinberg, R. L.; Kenyon, W. E.; Mitra, P. P. *J. Magn. Reson. A* **1994**, *108*, 206.
(10) Cheah, K. Y.; Chiaranussati, N.; Hollewand, M. P.; Gladden, L. F. *Appl. Catal. A: General* **1994**, *115*, 147.
(11) Packer, K. J. *Prog. NMR Spectrosc.* **1967**, *3*, 87.
(12) Foley, I.; Farooqui, S. A.; Kleinberg, R. L. *J. Magn. Reson. A* **1996**, *123*, 95.